UDC 547
DOI: 10.15587/1729-4061.2020.217282

DEVELOPMENT OF COBALT-FREE OXIDE ($SM_{0.5}SR_{0.5}FE_{0.8}CR_{0.2}O_{3-\delta}$) CATHODE FOR INTERMEDIATE-TEMPERATURE SOLID OXIDE FUEL CELLS (IT-SOFCS)

Iwan Susanto
Doctor of Materials Science and Engineering, Assistance Professor*
E-mail: iwan.susanto@mesin.pnj.ac.id
Dianta Mustofa Kamal
Doctor of Energy Conversion, Assistance Professor*
Sidiq Ruswanto
Master of Materials Science and Engineering*
Rahmat Subarkah
Master of Thermo Fluids Engineering, Assistance Professor*
Fuad Zainuri
Doctoral Candidate of Mechanical Engineering, Assistance Professor*
Sulaksana Permana
Doctor of Engineering in Metallurgy and Materials**
Johny Wahyuadi Soedarsono
Doctor of Engineering, Professor**
Adi Subardi
Doctor of Materials Science and Engineering, Assistance Professor
Department of Mechanical Engineering
Institut Teknologi Nasional Yogyakarta
Jl. Babarsari, Tambak Bayan, Caturtunggal, Kec. Depok,
Kabupaten Sleman, Daerah Istimewa Yogyakarta, Indonesia, 55281
Yen-Pei Fu
Doctor of Materials, Professor
Department of Materials Science and Engineering
National Dong Hwa University
Shoufeng Township, Hualien, Taiwan, 974301
*Department of Mechanical Engineering
Politeknik Negeri Jakarta
Kukusan, Beji, Depok, Indonesia, 16425
**Centre of Mineral Processing and Corrosion Research
Department of Metallurgy and Materials
Universitas Indonesia
Depok, Jawa Barat, Indonesia, 16424

A cobalt-free perovskite oxide $Sm_{0.5}Sr_{0.5}Fe_{0.8}Cr_{0.2}O_{3-\delta}$ (SSFC) has been exploited as a novel cathode for intermediate-temperature solid oxide fuel cells (IT-SOFCs). The cathode model was synthesized with the addition of the chromium element in the B side of the composite metallic oxide system, which was then formed by the solid-state reaction method. The model system was further characterized in detail for getting the properties behavior. The solid-state reaction of the SSFC system was observed through thermal gravimetric analysis. Meanwhile, the structural properties were investigated by x-ray diffraction, and the weight loss was examined by the thermal gravimetric analysis as well. Furthermore, the thermal expansion coefficient was determined by the thermal-mechanical analysis, and the conductivity properties were tested by the thermal conductivity analysis. The result showed that the SSFC cathode demonstrated the crystalline structure based on the design with a perovskite phase. The oxygen content created on the model structure was obtained to be 2.98 after the calcination process. The average thermal expansion coefficient was achieved up to 5.0×10^{-6} K^{-1} as the heating given up to 800 °C. Moreover, the conductivity value reached from 2 $S\cdot cm^{-1}$ at 400 °C and it increased to be a maximum of 7.5 $S\cdot cm^{-1}$ at 700 °C. In addition, the presence of Cr^{6+} cation valence coordinated with the oxygen anion could lead to generating a large concentration of oxygen vacancies on the cathode surface, facilitating the transport of the O^{2-} anion in the cathode system. Based on these results, the SSFC cathode has good properties as a composite system promising for IT-SOFCs application in the future

Keywords: solid oxide fuel cells, cobalt-free cathode, perovskite structure, oxygen content, conductivity

Received date 09.10.2020
Accepted date 14.11.2020
Published date 29.12.2020

1. Introduction

Intermediate-temperature SOFCs (IT-SOFCs) have attracted a great deal of attention as potential power generators due to the high efficiency, low environmental impact, and fuel versatility [1–3]. Among perovskite-type oxides noted as $ABO_{3-\delta}$, mixed ionic and electronic conductors (MIEC) have been widely used in IT-SOFCs [4–8]. They are good materials for important applications, including as electro-catalysts for solid oxide fuel cells (SOFCs), in oxygen-permeable membranes, and in oxygen absorbers. Some studies have reported that the MIEC cathode demonstrated high performance electro-catalytic activities, excellent oxygen transport and surface exchange properties, and consequently high electrochemical activities [9–14]. However, as in practice for a long-term application, these Co-based MIECs have low stability influenced by the difference of high thermal expansion with an electrolyte, which has challenged to develop the cathode for IT-SOFCs. Moreover, a high cost of Co compared to other rare metals is also another thing to be considered for effective application [15]. Therefore, a comprehensive study is needed to find out a novel cathode for intermediate-temperature solid oxide fuel cells (IT-SOFCs) to overcome the various limitations above. The use of another material, including the chromium element as the metal transition for the cathode system could be a smart strategy to the development of the IT-SOFCs system [16]. The development of IT-SOFCs has also made it preferable to use metallic interconnects (MICs) to reduce the cost and significantly increase efficiency.

2. Literature review and problem statement

Recently, impressive studies have been devoted to exploring the free Co-based cathode to overcome several issues for applying the IT-SOFCs [15–18]. The use of the Fe element in the B side of the cathode system as the Fe-based composite oxides is expected to be low-cost and more stable under SOFC operation conditions (500 to 800 °C and air atmosphere), which is due to the stable electronic configuration of the Fe ions [19, 20]. Up to now, the model system is continually developing in the B side of the Fe-based perovskite oxides to get excellent performance in the cathode system. The extensive work has been reported using the metal transition for improving the B-side of perovskite structure [21–25]. The addition of the Cr element in the perovskite oxides contains a high valence transition, which is stable over a wide range of oxygen partial pressure pO_2 values [26]. Even more interesting, the Cr-doped Fe in the B-side of perovskite structure leads to the best performance for the cathode material of SOFCs. The use of Cr^{6+} cation valence coordinated with the oxygen anion, producing a large concentration of oxygen vacancies on the surface of the cathode system [27]. Moreover, the more oxygen vacancies present, the more rapidly oxygen can be absorbed and separating reduced on the surface, and then move into an oxide lattice for a given chemical potential driving force. In addition, Cr co-doped in electrolyte also shows better ionic conductivity, which increases ionic transfer from cathode to anode elements during operation [28]. Unfortunately, the analysis of the cobalt-free cathode based on the Cr doped Fe ions in the B-site mixed with the Sm and Sr element in the A-site of the composite system have been not explored yet. So, in this work, we schematically investigated the structure and properties of the cobalt-free cathode based on the composite materials of Sm, Sr, Fe, and Cr for potential application in IT-SOFCs. Several characterizations and analysis will be conducted to investigate the properties of the cathode model in more detail.

3. The aim and objectives of the study

The aim of the study is to investigate the properties of cobalt-free perovskite oxide ($Sm_{0.5}Sr_{0.5}Fe_{0.8}Cr_{0.2}O_{3-\delta}$) cathode for IT-SOFC$_S$.

To achieve this aim, the following objectives are accomplished:

– modification of the perovskite structure with the addition of the Cr element in the B side to be a composite cathode of SSFC using the solid-state reaction method;

– characterization and testing of the structure of composite metal oxide and performing the model system of SSFC cathode.

4. Materials and methods of the study of cobalt-free perovskite oxide ($Sm_{0.5}Sr_{0.5}Fe_{0.8}Cr_{0.2}O_{3-\delta}$) cathode for IT-SOFC$_S$

The SSFC cathodes are prepared conventionally using the solid-state reaction method. A stoichiometric amount of metallic oxide composite of Sm_2O_3, $SrCO_3$, Fe_2O_3, and CrO material was dissolved and mixed with an alcohol solution for 12 hours using zirconia balls. The precipitate powders were further dried in the oven at 80 °C for 24 hours. The obtained precursor powders of SSFC were calcined under air atmosphere at 1,000 °C for 4 hours with a heating rate of 3 °C min^{-1} and natural cooling in the furnace. Further, the calcination powder was ground with an agate mortar and screened at 400 mesh. The powders were further pressed into a square bulk with a size of 5×7×10 mm and a cylindrical one with a diameter of 5 mm and a length of 10 mm. Two types of bulk were then sintered at 1,200 °C for 4 hours with a heating rate of 3 °C min^{-1} and natural cooling in the furnace. The crystal structure of the cathode powder was characterized using XRD. The thermogravimetric (TG) analysis of the powders related to weight loss is performed on thermal derivatives for a heating rate of 10 °C min^{-1}. In addition, two kinds of bulk samples were then measured to determine both the electrical conductivity and the coefficient of thermal expansion.

5. Results

5. 1. Modification of the structure of SSFC cathode

Thermal Gravimetric Analysis.

Fig. 1, *a* shows the curves of both Differential Thermal Analysis (DTA) and Thermogravimetric (TG) Analysis of SSFC oxide powders, which were calcined from the room temperature to 1,200 °C. There are three steep valleys on the curve (DTA) attended at 295 °C, 430 °C, and 900 °C for point *A*, *B* and *C*, serially. As well as on the TG curve, the decreasing curve was also drastically created at the same location, namely started from point 1 to 5, respectively.

Fig. 1, *b* displays the curve of the DTA and TG analysis of samarium oxide powder, which was heated from room temperature to 1,200 °C. There are two steep valleys on the curve attended at 300 °C and 452 °C for point A and B of DTA. As well as the TG curve, the decreasing curve was also drastically created around the same location.

Fig. 2 demonstrates the thermal gravimetric curve of the SSFC cathode material after the calcination process observed from room temperature to 1,000 °C. The y-axis shows the percentage of TG (%) of SSFC material during the heating process. The thermal gravimetric curve demonstrated the behavior of weight loss of cathode materials.

The exhibiting curve in Fig. 2 started from point *A* at 25 °C and was stable up to 150 °C. The curve was further going to decrease to 0.03 % TG at 380 °C (point *B* to C). Finally, the curve drop was drastically along point *C*–*D* with a decrease of 0.17 % TG as the temperature reached up to 900 °C. Meanwhile, the curve was further stable after this temperature to 1,000 °C.

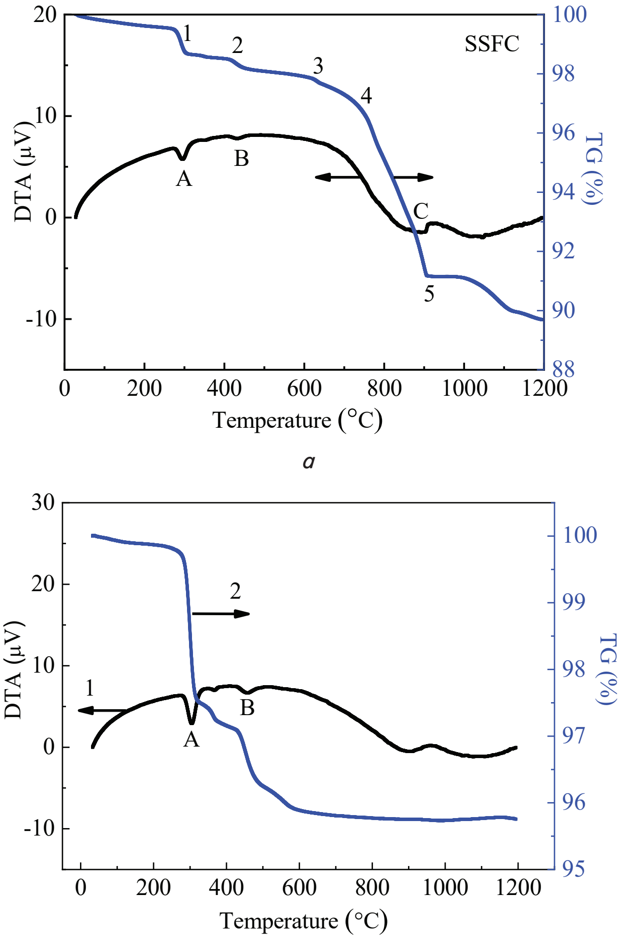

a

b

Fig. 1. Differential Thermal Analysis (DTA) and Thermogravimetric (TG) Analysis for: *a* — SSFC cathode powders, *b* — samarium oxide powders

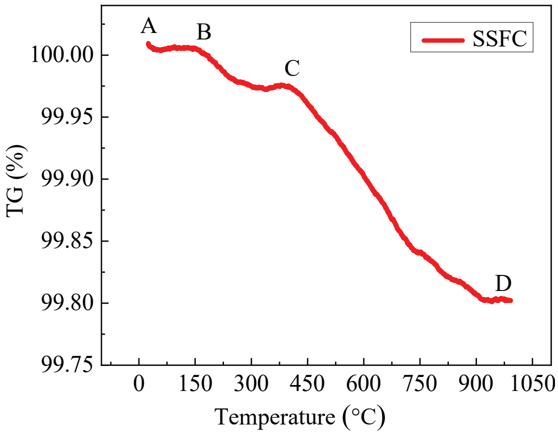

Fig. 2. Thermal gravimetric curve of SSFC composite cathode

5. 2. Characterization and testing of SSFC cathode

Structure Analysis.

Fig. 3 shows the XRD pattern of the SSFC powder structure (*A*) calcined at 1,000 °C during 4 hours. While the perovskite structure (*B*) of lanthanum ferrite ($LaFeO_3$) was used as a reference. The characterization was carried out for observing as long as six degrees in 2θ.

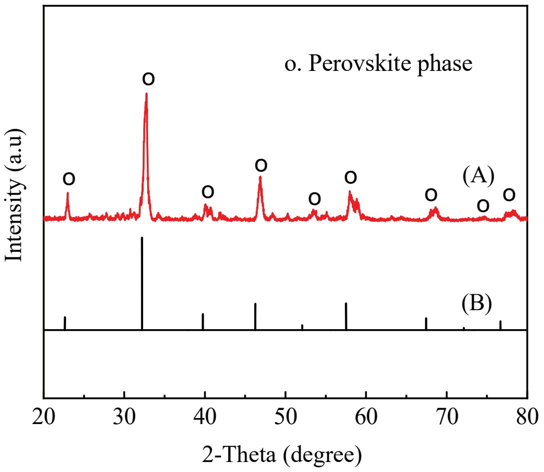

Fig. 3. XRD diffraction pattern of SSFC cathode

There are nine main peaks in the pattern with different intensity and broadening peak raised shown in Fig. 3 (*A*). Those peaks were located at 22.98°, 32.74°, 40.66°, 46.88°, 52.52°, 57.98°, 67.72°, 72.78°, and 77.44°. The peak position seems matched with the references of perovskite structure (*B*).

Oxygen Content Analysis.

Fig. 4 shows the oxygen content ($O_{3-\delta}$) formed in the SSFC cathode composite material after the calcination process. The observation of $O_{3-\delta}$ has been done from room temperature to 1,000 °C. The oxygen content of the model was designed using O_3 in the perovskite structure shown on the *y*-axis.

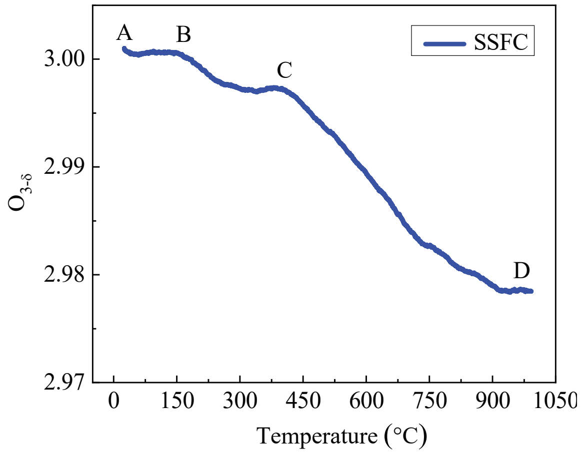

Fig. 4. Oxygen content of SSFC

The $O_{3-\delta}$ curve in Fig. 4 was noted from point *A* to *D* as the behavior of SSFC cathode materials. The trend of the displaying curve was similar to the TG analysis demonstrated in Fig. 2. The stable curve was in the *A* to *B* region, and the decreasing curve of 0.02 during 200 °C was located at point *B* to *C*. As well, the reduction curve was continually as long point C to D for 498 °C with the reduction of oxygen content of 0.22.

Thermal expansion coefficient measurement.

The coefficient of thermal expansion of the SSFC cathode is displayed in detail in Fig. 5. The heating temperature given to the sample ranges from room temperature to 850 °C.

While the expansion thermal value was recorded by the strain of the SSFC cathode in $\Delta L/Lo$ of 10^{-6} K^{-1} on the y-axis.

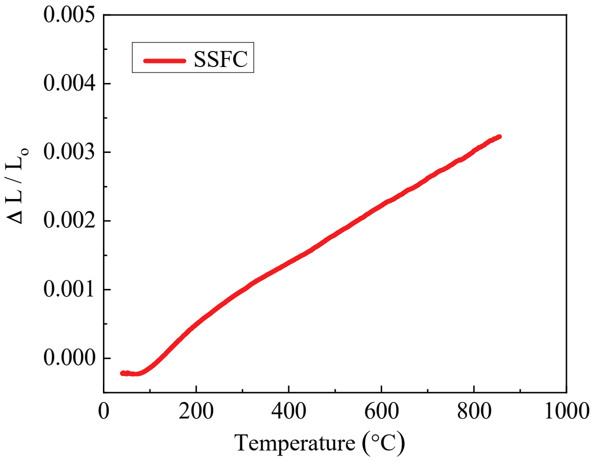

Fig. 5. Thermal expansion coefficient of SSFC cathode

Based on the result exhibited in Fig. 5, the curve was stable and the slope of the curve was just close to zero at low temperature. The increased strain of SSFC began as the temperature reached 140 °C. The initial strain of the curve pattern is a little bit parabolic and it subsequently becomes linear as the temperature increases up to the range of 300 to 850 °C. The average of the thermal coefficient of 4.7×10^{-6} K^{-1} at a temperature of 100–800 °C was obtained. Its value consists of 3.8×10^{-6} K^{-1} as the initial heating temperature is 100–300 °C and it becomes 5.0×10^{-6} K^{-1} at the temperature between 300–800 °C.

Conductivity properties.

Fig. 6 illustrated the curve related to the conductivity of the SSFC cathode composite materials. The performance was carried out in the temperature range of 400 to 800 °C under atmospheric air pressure with an oxygen content of 0.21 atm (21 % O_2). The conductivity value was shown on the y-axis with $S\cdot cm^{-1}$ unit.

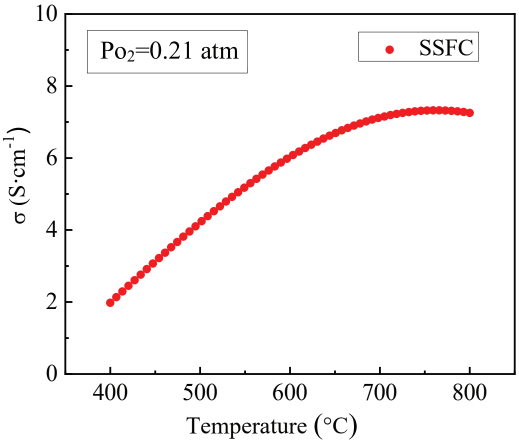

Fig. 6. Conductivity of SSFC cathode composite materials for SOFC

The trend curve shown in Fig. 6 was exhibited by the conductivity value recorded in the beginning value of 2 $S\cdot cm^{-1}$. The parabolic curve was demonstrated by the increasing temperature. The conductivity value increased regularly up to 7.25 $S\cdot cm^{-1}$ at 800 °C, and it reached to be a maximum of 7.32 $S\cdot cm^{-1}$ at 766 °C. As the temperature increased, the curve was regularly reduced.

6. Discussion of experimental results

For the thermal gravimetric curve shown in Fig. 1, *a*, the calcination process of composite powders was carried out to generate the solid-state reaction of the model system. The decrease of the TG curve for number 1 to 5 was related to the reduction of weigh loss of powders. The reduction of the curve at the first phase occurred in the range of 150–380 °C for the calcination process [30]. It could be evaporated water content contained in the SSFC powders due to the heat energy given by the system. The evaporated water content was also demonstrated by the samarium powder, which was performed by the weight loss in the temperature range shown in Fig. 1, *b*. It was also proven by the endothermic peak at the same temperature due to the dehydration of materials. Meanwhile, at point 3 around 600 °C in Fig. 1, *a*, the weight loss happened was believed that evaporating was dominated from the impurity of samarium material confirmed in Fig. 1, *b*. While, at the point of 4 to 5, the rate of subsequent weight loss occurs due to the decomposition of strontium carbonate up to oxide materials of SSFC. The solid-state reaction was created on the SSFC, which was held from this temperature up to 900 °C [31]. So, the total weight loss of SSFC powders during the calcination process reached up to 9 %. In addition, the endothermic reaction further will generate the formation of the perovskite structure, which was confirmed by XRD characterization in Fig. 3. Moreover, the decrease of the oxygen content shown in Fig. 4 was affected by the heat energy given by the system. Heat energy could encourage the reduction reaction at the oxygen levels decreased to 2.98 of $O_{3-\delta}$ for the perovskite structure in the SSFC cathode. The decreased oxygen content as an increase in temperature could facilitate the transport of the mobility oxygen to be easier in the cathode system as it was applied in the IT-SOFC system.

To get a deep understanding of the crystalline structure formed, the XRD pattern is demonstrated in detail for the SSFC cathode. The main nine peaks with different intensity at several theta positions related to the crystalline structure used on the XRD pattern are shown in Fig. 3 (A). The crystalline structure exhibited the perovskite-phase constructed on the composite model system. The structure of the phase is also similar to a nearly cubic structure of $LaFeO_3$ in Fig. 3 (*A*) [29], indicating that the crystalline structure with the perovskite phase was formed on the SSFC cathode. This structure corresponded to the initial design in the perovskite phase for the SSFC cathode materials event the Cr element added on the B-side of the model system. Based on the XRD pattern above, the stoichiometry of composite metal oxide for the SSFC cathode materials could be constructed the crystalline structure with the perovskite-phase through the solid-state reaction method.

Furthermore, the thermal strain of the SSFC cathode is shown clearly in Fig. 5. Low thermal strain of 5.0×10^{-6} K^{-1} was demonstrated by the model system, indicating that it has a small expansion coefficient compared to the SDC electrolyte, 12.6×10^{-6} K^{-1} [32]. However, a large enough difference in the thermal expansion coefficient between the SSFC cathode and SDC electrolyte might reduce the performance for long-term applications. The thermal expansion behavior is important for the thermal compatibility of the cathode with the electrolyte or interlayer in the SOFCs system. It also contributes to the interface resistance in electrochemical performance as well as the long-term stability of the cathode [33]. According to the test result, the curve increased with raising temperature. This could be due to the lattice expansion of the oxides induced by the weakening of the electrostatic attractive force between anions (O^{2-}) and thermally reduced cations at elevated temperature [29]. Moreover, the slope of the curves increases at a higher temperature because of the loss of oxygen in the SSFC cathode.

In addition, the conductivity of SSFC is the sum of the electronic and ionic conductivity, which was associated with the electronic hole and the oxygen vacancy in the structure. The increase in conductivity at lower temperatures is associated with the transfer of thermally activated electrons by jumping through the Fe^{4+}–O–Fe^{3+} and Cr^{3+}–O–Cr^{6+} bonds [33, 34], whereas the decrease in conductivity above 766 °C is related to the decrease of electronic hole concentration through thermal reduction of Fe^{4+}, Fe^{3+}, as well as the formation of more oxygen vacancies. Moreover, the use of Cr^{6+} cation valence coordinated with the oxygen anion, producing a large concentration of oxygen vacancies on the surface of the cathode system, which facilitated the transport of O^{2-} in the SSFC cathode system. Based on the thermal strain analysis, it takes a stoichiometry Cr composition on the B-side to produce a close match of the thermal expansion coefficient compared to the SDC electrolyte. In addition, further studies are needed for investigating the performance of SSFCs as was integrated with the electrolyte and cathode in a single cell.

7. Conclusions

1. The composite structure of the SSFC cathode has been successfully modified by the solid-state reaction method. The perovskite structure was constructed with the addition of the Cr element in the B side of the SSFC system.

2. The characterization and testing results of the SSFC system demonstrated that the thermal gravimetric reported a weight reduction of 0.2 % for SSFC cathode materials associated with oxygen losses during the heating process. Low thermal expansion coefficient of 4.7×10^{-6} K^{-1} for the model system was also exhibited by the thermal-mechanical analysis. Thus, good conductivity properties related to the performance of SSFC cathode were obtained to be a maximum of 7.32 $S\cdot cm^{-1}$ at 766 °C.

Acknowledgments

The authors are grateful to the financial support provided by Unit Penelitian dan Pengabdian Masyarakat, Politeknik Negeri Jakarta (UP2M-PNJ) under contract number: B.150/PL3.18/PN.00.03/2020 that made this work possible. The authors are also grateful for the financial support of this research by the Ministry of Science and Technology of Taiwan under contract number: MOST 106-2113-M-259-011.

References

1. Wakui, T., Yokoyama, R., Shimizu, K. (2010). Suitable operational strategy for power interchange operation using multiple residential SOFC (solid oxide fuel cell) cogeneration systems. Energy, 35 (2), 740–750. doi: https://doi.org/10.1016/j.energy.2009.09.029
2. Fernandes, A., Woudstra, T., van Wijk, A., Verhoef, L., Aravind, P. V. (2016). Fuel cell electric vehicle as a power plant and SOFC as a natural gas reformer: An exergy analysis of different system designs. Applied Energy, 173, 13–28. doi: https://doi.org/10.1016/j.apenergy.2016.03.107
3. Naimaster, E. J., Sleiti, A. K. (2013). Potential of SOFC CHP systems for energy-efficient commercial buildings. Energy and Buildings, 61, 153–160. doi: https://doi.org/10.1016/j.enbuild.2012.09.045
4. Song, X., Le, S., Zhu, X., Qin, L., Luo, Y., Li, Y. et. al. (2017). High performance $BaFe_{1-x}BixO_{3-\delta}$ as cobalt-free cathodes for intermediate temperature solid oxide fuel cells. International Journal of Hydrogen Energy, 42 (24), 15808–15817. doi: https://doi.org/10.1016/j.ijhydene.2017.05.061
5. Zhu, M., Cai, Z., Xia, T., Li, Q., Huo, L., Zhao, H. (2016). Cobalt-free perovskite $BaFe_{0.85}Cu_{0.15}O_{3-\delta}$ cathode material for intermediate-temperature solid oxide fuel cells. International Journal of Hydrogen Energy, 41 (8), 4784–4791. doi: https://doi.org/10.1016/j.ijhydene.2016.01.071
6. Yao, C., Zhang, H., Liu, X., Meng, J., Meng, J., Meng, F. (2019). A niobium and tungsten co-doped $SrFeO_{3-\delta}$ perovskite as cathode for intermediate temperature solid oxide fuel cells. Ceramics International, 45 (6), 7351–7358. doi: https://doi.org/10.1016/j.ceramint.2019.01.019
7. Yang, H., Gu, Y., Zhang, Y., Zheng, Y., Zhang, Z., Ge, L. et. al. (2019). Sr-substituted $SmBa_{0.75}Ca_{0.25}CoFeO_{5+\delta}$ as a cathode for intermediate-temperature solid oxide fuel cells. Journal of Alloys and Compounds, 770, 616–624. doi: https://doi.org/10.1016/j.jallcom.2018.08.143
8. Liu, H., Zhu, K., Liu, Y., Li, W., Cai, L., Zhu, X. et. al. (2018). Structure and electrochemical properties of cobalt-free perovskite cathode materials for intermediate-temperature solid oxide fuel cells. Electrochimica Acta, 279, 224–230. doi: https://doi.org/10.1016/j.electacta.2018.05.086
9. Subardi, A., Chen, C.-C., Cheng, M.-H., Chang, W.-K., Fu, Y.-P. (2016). Electrical, thermal and electrochemical properties of $SmBa_{1-x}Sr_xCo_2O_{5+\delta}$ cathode materials for intermediate-temperature solid oxide fuel cells. Electrochimica Acta, 204, 118–127. doi: https://doi.org/10.1016/j.electacta.2016.04.069
10. Zhao, L., He, B., Zhang, X., Peng, R., Meng, G., Liu, X. (2010). Electrochemical performance of novel cobalt-free oxide $Ba_{0.5}Sr_{0.5}Fe_{0.8}Cu_{0.2}O_{3-\delta}$ for solid oxide fuel cell cathode. Journal of Power Sources, 195 (7), 1859–1861. doi: https://doi.org/10.1016/j.jpowsour.2009.09.078
11. Li, C.-H., Hu, S.-H., Tay, K.-W., Fu, Y.-P. (2012). Electrochemical characterization of gradient $Sm_{0.5}Sr_{0.5}CoO_{3-\delta}$ cathodes on $Ce_{0.8}Sm_{0.2}O_{1.9}$ electrolytes for solid oxide fuel cells. Ceramics International, 38 (2), 1557–1562. doi: https://doi.org/10.1016/j.ceramint.2011.09.041

12. Javed, M. S., Shaheen, N., Idrees, A., Hu, C., Raza, R. (2017). Electrochemical investigations of cobalt-free perovskite cathode material for intermediate temperature solid oxide fuel cell. International Journal of Hydrogen Energy, 42 (15), 10416–10422. doi: https://doi.org/10.1016/j.ijhydene.2017.02.045
13. Ling, Y., Zhang, X., Wang, Z., Wang, S., Zhao, L., Liu, X., Lin, B. (2013). Potentiality of cobalt-free perovskite $Ba_{0.5}Sr_{0.5}Fe_{0.9}Mo_{0.1}O_{3-\delta}$ as a single-phase cathode for intermediate-to-low-temperature solid oxide fuel cells. International Journal of Hydrogen Energy, 38 (33), 14323–14328. doi: https://doi.org/10.1016/j.ijhydene.2013.08.089
14. Subardi, A., Liao, K.-Y., Fu, Y.-P. (2019). Oxygen transport, thermal and electrochemical properties of $NdBa_{0.5}Sr_{0.5}Co_2O_{5+\delta}$ cathode for SOFCs. Journal of the European Ceramic Society, 39 (1), 30–40. doi: https://doi.org/10.1016/j.jeurceramsoc.2018.01.022
15. Baharuddin, N. A., Muchtar, A., Somalu, M. R. (2017). Short review on cobalt-free cathodes for solid oxide fuel cells. International Journal of Hydrogen Energy, 42 (14), 9149–9155. doi: https://doi.org/10.1016/j.ijhydene.2016.04.097
16. Baharuddin, N. A., Muchtar, A., Somalu, M. R., Kalib, N. S., Raduwan, N. F. (2019). Synthesis and characterization of cobalt-free $SrFe_{0.8}Ti_{0.2}O_{3-\delta}$ cathode powders synthesized through combustion method for solid oxide fuel cells. International Journal of Hydrogen Energy, 44 (58), 30682–30691. doi: https://doi.org/10.1016/j.ijhydene.2018.11.142
17. Meng, X., Lü, S., Yu, W. W., Ji, Y., Sui, Y., Wei, M. (2018). Layered perovskite $LnBa_{0.5}Sr_{0.5}Cu_2O_{5+\delta}$ (Ln=Pr and Nd) as cobalt-free cathode materials for solid oxide fuel cells. International Journal of Hydrogen Energy, 43 (9), 4458–4470. doi: https://doi.org/10.1016/j.ijhydene.2018.01.033
18. Ding, X., Gao, X., Zhu, W., Wang, J., Jiang, J. (2014). Electrode redox properties of $Ba_{1-x}La_xFeO_{3-\delta}$ as cobalt free cathode materials for intermediate-temperature SOFCs. International Journal of Hydrogen Energy, 39 (23), 12092–12100. doi: https://doi.org/10.1016/j.ijhydene.2014.06.009
19. Yin, J.-W., Yin, Y.-M., Lu, J., Zhang, C., Minh, N. Q., Zhang, W., Ma, Z.-F. (2014). $Nd_{0.5}Sr_{0.5}Fe_{0.8}Cu_{0.2}O_{3-\delta}$–$xSm_{0.2}Ce_{0.8}O_{1.9}$ cobalt-free composite cathodes for intermediate temperature solid oxide fuel cells. International Journal of Hydrogen Energy, 39 (31), 17852–17856. doi: https://doi.org/10.1016/j.ijhydene.2014.08.131
20. He, Z., Xia, L., Chen, Y., Yu, J., Huang, X., Yu, Y. (2015). Layered perovskite $Sm_{1-x}La_xBaFe_2O_{5+\delta}$ as cobalt-free cathodes for IT-SOFCs. RSC Advances, 5 (71), 57592–57598. doi: https://doi.org/10.1039/c5ra09762b
21. Baharuddin, N. A., Mohd Nazrul Aman, N. A., Muchtar, A., Somalu, M. R., Abdul Samat, A., Aznam, M. I. (2019). Structural, morphological, and electrochemical behavior of titanium-doped $SrFe_{1-x}Ti_xO_{3-\delta}$ (x=0.1–0.5) perovskite as a cobalt-free solid oxide fuel cell cathode. Ceramics International, 45 (10), 12903–12909. doi: https://doi.org/10.1016/j.ceramint.2019.03.216
22. Cai, H., Zhang, L., Xu, J., Huang, J., Wei, X., Wang, L. et. al. (2019). Cobalt–free $La_{0.5}Sr_{0.5}Fe_{0.9}Mo_{0.1}O_{3-\delta}$ electrode for symmetrical SOFC running on H_2 and CO fuels. Electrochimica Acta, 320, 134642. doi: https://doi.org/10.1016/j.electacta.2019.134642
23. Chen, M., Paulson, S., Kan, W. H., Thangadurai, V., Birss, V. (2015). Surface and bulk study of strontium-rich chromium ferrite oxide as a robust solid oxide fuel cell cathode. Journal of Materials Chemistry A, 3 (45), 22614–22626. doi: https://doi.org/10.1039/c5ta05815e
24. Niu, Y., Lv, W., Chen, D., Han, J., He, W. (2019). A model study on correlation between microstructure-gas diffusion and Cr deposition in porous LSM/YSZ cathodes of solid oxide fuel cells. International Journal of Hydrogen Energy, 44 (33), 18319–18329. doi: https://doi.org/10.1016/j.ijhydene.2019.05.115
25. Parveen, I. M., Asvini, V., Saravanan, G., Ravichandran, K., Kalaiselvi, D. (2019). Deficiency of O_2 molecules enhances ionic conductivity in Cr-doped O-Ce-O for solid oxide fuel cell applications. Ceramics International, 45 (10), 13127–13137. doi: https://doi.org/10.1016/j.ceramint.2019.03.247
26. Lu, J., Yin, Y.-M., Yin, J., Li, J., Zhao, J., Ma, Z.-F. (2015). Role of Cu and Sr in Improving the Electrochemical Performance of Cobalt-Free $Pr_{1-x}Sr_xFe_{1-y}Cu_yO_{3-\delta}$ Cathode for Intermediate Temperature Solid Oxide Fuel Cells. Journal of The Electrochemical Society, 163 (2), F44–F53. doi: https://doi.org/10.1149/2.0181602jes
27. Zhang, C., Zhao, H. (2012). A novel cobalt-free cathode material for proton-conducting solid oxide fuel cells. Journal of Materials Chemistry, 22 (35), 18387. doi: https://doi.org/10.1039/c2jm32627b
28. Yin, J.-W., Yin, Y.-M., Lu, J., Zhang, C., Minh, N. Q., Ma, Z.-F. (2014). Structure and Properties of Novel Cobalt-Free Oxides $Nd_xSr_{1-x}Fe_{0.8}Cu_{0.2}O_{3-\delta}$ ($0.3 \le x \le 0.7$) as Cathodes of Intermediate Temperature Solid Oxide Fuel Cells. The Journal of Physical Chemistry C, 118 (25), 13357–13368. doi: https://doi.org/10.1021/jp500371w
29. Yin, S., Li, M., Zeng, Y., Li, C., Chen, X., Ye, Z. (2014). Study of $Sm_{0.2}Ce_{0.8}O_{1.9}$ (SDC) electrolyte prepared by a simple modified solid-state method. Journal of Rare Earths, 32 (8), 767–771. doi: https://doi.org/10.1016/s1002-0721(14)60138-1
30. Li, S., Lü, Z., Huang, X., Su, W. (2008). Thermal, electrical, and electrochemical properties of Nd-doped $Ba_{0.5}Sr_{0.5}Co_{0.8}Fe_{0.2}O_{3-\delta}$ as a cathode material for SOFC. Solid State Ionics, 178 (35-36), 1853–1858. doi: https://doi.org/10.1016/j.ssi.2007.11.016
31. Chen, M., Paulson, S., Thangadurai, V., Birss, V. (2013). Sr-rich chromium ferrites as symmetrical solid oxide fuel cell electrodes. Journal of Power Sources, 236, 68–79. doi: https://doi.org/10.1016/j.jpowsour.2013.02.024